1-15-2016

The common genetic influence over processing speed and white matter microstructure: Evidence from the Old Order Amish and Human Connectome Projects

Peter Kochunov

Paul M. Thompson

Anderson M. Winkler
The University of Texas Rio Grande Valley, Anderson.Winkler@utrgv.edu

Mary Morrissey

Mao Fu

See next page for additional authors

Authors

Peter Kochunov, Paul M. Thompson, Anderson M. Winkler, Mary Morrissey, Mao Fu, Thomas R. Coyle, Xiaoming Du, Florian Muellerklein, Anya Savransky, and Christopher Gaudiot

The common genetic influence over processing speed and white matter microstructure: Evidence from the Old Order Amish and Human Connectome Projects

Peter Kochunov[1],[*], **Paul M. Thompson**[2], **Anderson Winkler**[3], **Mary Morrissey**[4], **Mao Fu**[4], **Thomas R. Coyle**[5], **Xiaoming Du**[1], **Florian Muellerklein**[1], **Anya Savransky**[1], **Christopher Gaudiot**[1], **Hemalatha Sampath**[1], **George Eskandar**[1], **Neda Jahanshad**[2], **Binish Patel**[1], **Laura Rowland**[1], **Thomas E Nichols**[6], **Jeffrey R. O'Connell**[4], **Alan R. Shuldiner**[4], **Braxton D. Mitchell**[4],[7], and **L. Elliot Hong**[1]

[1] Maryland Psychiatric Research Center, Department of Psychiatry, University of Maryland School of Medicine, Baltimore, MD, USA.

[2] Imaging Genetics Center, Keck School of Medicine of USC, Marina del Rey, CA, USA

[3] FMRIB Centre, Oxford University, Oxford, UK

[4] Department of Medicine, University of Maryland School of Medicine, Baltimore, MD, USA.

[5] Department of Psychology, University of Texas at San Antonio, San Antonio, TX.

[6] Department of Statistics, University of Warwick, Warwick, UK

[7] Geriatrics Research and Education Clinical Center, Baltimore Veterans Administration Medical Center, Baltimore, MD 21201, USA.

Abstract

Speed with which brain performs information processing influences overall cognition and is dependent on the white matter fibers. To understand genetic influences on processing speed and white matter FA, we assessed processing speed and diffusion imaging fractional anisotropy (FA) in related individuals from two populations. Discovery analyses were performed in 146 individuals from large Old Order Amish (OOA) families and findings were replicated in 485 twins and siblings of the Human Connectome Project (HCP). The heritability of processing speed was h^2=43% and 49% (both p < 0.005), while the heritability of whole brain FA was h^2=87% and 88% (both p < 0.001), in the OOA and HCP, respectively. Whole brain FA was significantly correlated with processing speed in the two cohorts. Quantitative genetic analysis demonstrated a significant degree to which common genes influenced joint variation in FA and brain processing speed. These estimates suggested common sets of genes influencing variation in both phenotypes, consistent

[*]Please address correspondence to: Dr. Peter Kochunov, Maryland Psychiatric Research Center, Department of Psychiatry, University of Maryland, School of Medicine, Baltimore, MD, USA, **Phone:** (410) 402-6110, **Fax** : (410)-402-7198, pkochunov@mprc.umaryland.edu.

with the idea that common genetic variations contributing to white matter may also support their associated cognitive behavior.

Introduction

Information processing is a fundamental cognitive function that supports the higher cognitive and behavior attributes, including working memory, executing function and others (Bartzokis et al., 2008; Salthouse, 2009). Speed with which brain processes information follows an inverse U-trend across the lifespan. It rises during maturation, reaches peak in the 3rd and 4th decades of life, after which point there is an age-related decline (Bartzokis et al., 2008; Salthouse, 2009). A life-span curve for the cerebral myelination mirrors this trend (Bartzokis et al., 2008; Flechsig, 1901; Kochunov et al., 2012). Myelination of the neuronal axons in the cerebral white matter is associated with a ten-fold higher signal transmission speed compared to unmyelinated axons and thirty-fold lower time needed for axonal repolarization to support signal transmission(Felts et al., 1997; Waxman and Bennett, 1972). WM supports cognitive and motor functions by facilitating the exchange of information across spatially distributed neural networks. We hypothesize that genetic contributions to white matter FA should have shared genetic control over neurocognitive processing speed performance. Toward that end, we use diffusion tensor imaging (DTI) methods to provide an in vivo measure of changes in white matter microstructure indexed by fractional anisotropy (FA) of water diffusion.

DTI-FA describes the directional selectivity of the random diffusion of water molecules (Basser, 1994; Conturo et al., 1996; Pierpaoli and Basser, 1996; Ulug et al., 1995). It is not a direct measurement of either myelination or white matter integrity(Jones et al., 2013). Instead, FA is sensitive to the anisotropy of the water diffusion created by the barrier of cellular membranes. For example, higher FA values (maximum theoretical value is 1.0) correspond to heavily myelinated WM tracts. The myelin layer of the axonal cell membranes hinders the diffusion of water molecules in all except the direction along the fiber tract, therefore producing highly anisotropic water diffusion estimates (Pierpaoli and Basser, 1996). Conversely, FA values are closer to zero for tissue where the water molecule motion is random and isotropic, such CSF. Thus, the absolute WM FA values are sensitive to many parameters including regional myelination levels, the degree of intra-voxel fiber crossing, axonal density and average axonal diameter (Beaulieu, 2002; Jones et al., 2013).

The neuroimaging research suggests a link between white matter FA and processing speed in healthy subjects. Among research findings linking neuroimaging measurements to variance in cognition, the strongest association was observed between white matter FA values and other proxy-measurements of white matter microstructure and fiber organization and the neurocognitive processing speed (Bartzokis, 2004; Bartzokis et al., 2008; Charlton et al., 2009; Karbasforoushan et al., 2015; Kennedy and Raz, 2009; Kochunov et al., 2009a; Kochunov et al., 2009b; Konrad et al., 2009; Muetzel et al., 2008; Schiavone et al., 2009; Vernooij et al., 2009). The overall conclusion of these studies was that white matter microstructure as indexed by FA and other neuroimaging indices are associated with the speed of cerebral information processing (Bartzokis et al., 2010). This link between white

matter FA and processing speed is consistent and replicable (Glahn et al., 2013; Penke et al., 2010; Wright et al., 2015). Moreover a consistent relationship between these measurements has also been observed in healthy subjects(Bartzokis et al., 2010; Kochunov et al., 2010; Vernooij et al., 2009) and in patients with heritable psychiatric disorders(Glahn et al., 2013; Karbasforoushan et al., 2015; Penke et al., 2010; Wright et al., 2015), giving a strong rationale to study the relationship for potential sources of shared genetic contributions.

A large proportion (40-80%) of the intersubject variance in the DTI-FA values(Braskie et al., 2011; Chiang et al., 2012; Chiang et al., 2009; Jahanshad et al., 2012; Jahanshad et al., 2010; Kochunov et al., 2015; Shen et al., 2014) and processing speed measurements(Glahn et al., 2011; Glahn et al., 2013) is explained by additive genetic factors. The high degree of genetic influence of these two traits posits them as important endophenotypes for genetic search for risk factors for heritable psychiatric disorders such as schizophrenia that are associated with both DTI-FA and processing speed deficits. This study aims for the first time to determine if shared genetic factors might partly explain the relationship between processing speed and white matter FA (Wright et al., 2015). We set out to (i) establish the degree of additive genetic contribution to processing speed and white matter FA phenotypes using a large pedigree cohort, (ii) test if effects replicate in an independent cohort, and (iii) to determine any regional tract-specificity of the shared genetic associations. Evidence that shared genetic factors influence white matter FA and processing speed may inform a more direct analytic approach for discovering influential genes in disorders that affect both phenotypes.

Toward these goals, we decomposed the phenotypic association between processing speed and FA into its genetic and environmental constituents using a family design with large pedigrees. The family study design offers a structure to test whether phenotypic variances are transmitted by inheritance of additive genetic variance. The Old Order Amish (OOA) are known for their very large family sizes, which include a large number of relatives and thus afford substantial power for genetic correlation analyses, even with a modest sample size. The OOA subjects are European Caucasian ancestry. They share similar rural upbringing and lifestyle that includes the same level of basic school education and virtually no illicit substance use. This relative environmental homogeneity in the OOA offers a rarely available setting to test shared heritability across different classes of phenotypes because environmental factors in the general population (for example substance abuse or differences in education levels) might impact each phenotype differently. Therefore, the OOA provides an interesting population-level control on heterogeneity and unmeasured sources of individual variation, making it easier to analyze the degree of shared heritability of traits.

Next we attempted to replicate the findings of shared genetic variance between DTI-FA and processing speed using an independent, genetically informative cohort - the publicly available twin-and-sibling based Human Connectome Project (HCP) dataset. In this dataset, both DTI-FA and processing speed (though measured differently than OOA) are available. Our hypothesis was that the two traits, white matter microstructure and processing speed, would show a consistent pattern of bivariate genetic association in both cohorts, despite the differences in population and methodological variability in data collection.

Methods

OOA Sample

Subjects—Brain imaging was conducted in 145 OOA Amish individuals (60M/85F, age=50.5±15.1; 18-75 years), in whom processing speed was measured in 85 (30M/55F, age=48.7±17.1; 18-75 years). All individuals were from seventeen nuclear families from Lancaster County, PA., who could be combined into a single large pedigree that connected them across eight generations based on genealogical records maintained by the OOA community and incorporated into the NIH Anabaptist Genealogy Database (AGDB) which traces back to the founders (Agarwala et al., 1999). Exclusion criteria included major medical and neurological conditions that might affect gross brain structures such as developmental disability, head trauma, seizure, stroke or transient ischemic attack. Subjects with type II diabetes and hypertension that were controlled with medications were included. Psychiatric conditions that were managed with medications were not excluded: the full sample (N=145) included 22 individuals with a lifetime diagnosis of psychiatric disorders, including mood disorders (n=8), anxiety disorders (n=10), psychosis (n=3), and other psychiatric disorders (n=1) based on the Structured Clinical Interview for DSM-IV Disorders (SCID). Among the subjects for whom processing speed measurements were available (N=85), there were 12 individuals with psychiatric disorders. Overall, this represented a 21.5% rate of psychiatric illness in the N=145 sample of the OOA isolate, comparable to the 22.4% prevalence rate of psychiatric illnesses in the general U.S. population (Kessler et al., 2005). All subjects with psychiatric disorders were taking psychotropic medications for their conditions. This included six subjects who were taking antipsychotics, thirteen subjects taking anti-depressants, eleven subjects taking mood-stabilizers and four subjects taking other psychotropic medications, with some subjects taking two medications. Heritability and genetic correlation analyses were performed by adding psychotropic medication status as a binary covariate. All subjects provided written informed consent on forms approved by the Institutional Review Board of University of Maryland Baltimore.

Processing speed measurements—Processing speed was assessed with the Digit Symbol Coding subtest of the WAIS-3, which is considered as a test for speed of information processing and psychomotor response (Wechsler, 1997). The task reports the number of correctly coded symbols within the two-minute interval. Besides processing speed, the task requires elements of attention, visuoperceptual processing, and working memory. Raw neuropsychological assessment scores were used, and corrections for age and sex were performed as part of the statistical modeling by including age, age^2, age $\times$ sex and $age^2 \times$ sex as covariates.

Imaging Protocol—The full protocol is detailed elsewhere(Kochunov et al., 2011). Briefly, all data was collected at the Maryland Psychiatric Research Center, using a 3T Siemens TRIO scanner equipped with a 32-channel phase array coil. The protocol consisted of a single-shot, echo-planar, single refocusing spin-echo, T2-weighted sequence with a spatial resolution of 1.7×1.7×3.0 mm. The sequence parameters were: TE/TR=87/8000 ms, FOV=200 mm, axial slice orientation with 50 slices and no gaps, 64 isotropically distributed

diffusion weighted directions, two diffusion weighting values (b=0 and 700 s/mm^2) and five b=0 images, calculated with an optimization technique that maximizes the contrast to noise ratio for FA measurements(Jones et al., 1999). The Generalized Autocalibrating Partially Parallel Acquisition (GRAPPA) acceleration procedure, with an acceleration factor of 2 and a 32-phase encoding reference line, was used in phase encoding direction. No acceleration along the Z-encoding direction was used. The total scan time was about 9 minutes. No cardiac or respiratory gating was used. The HARDI data were pre-processed with ENIGMA-DTI pipeline. Briefly, FMRIB Software Library (FSL) package, was used to perform the eddy-current and motion correction and calculate the fractional anisotropy (FA) images by fitting the diffusion tensor to the raw diffusion data, using default parameters (Smith SM, 2002). The quality of the data was inspected using QA/QC tools implemented in ENIGMA-DTI pipeline with all data passing the recommended checks.

HCP Sample

Subjects—Data were from 481 (194/287 M/F) participants from the Human Connectome Project (HCP) released in June 2014 (humanconnectome.org) after passing the HCP quality control and assurance standards (Marcus et al., 2013). Participants were recruited from the Missouri Family and Twin Registry (Van Essen et al., 2013). All HCP participants were from young adult sibships of average size 3–4 that include an MZ or DZ twin pair and the non-twin siblings. Subjects ranged in age from 22 to 36 years (29.1±3.5 years). This age range was chosen as it corresponds to a period after neurodevelopment is largely completed and before the typical age of onset of neurodegenerative changes. This release included 117 twin pairs (57 monozygotic and 60 dizygotic pairs), and 246 of their siblings. The full set of inclusion and exclusion criteria is detailed elsewhere (Van Essen et al., 2013). In short, the HCP subjects are healthy young adults within a restricted age range and free from major psychiatric or neurological illnesses (Edens et al., 2010; Sartor et al., 2010). All subjects provided written informed consent on forms approved by the Institutional Review Board of Washington University in St Louis.

Processing speed measurements—Processing speed was assessed using the NIH Toolbox Pattern Comparison Processing Speed (PCPS) Test (http://www.nihtoolbox.org) (Carlozzi et al., 2013). This test asks participants to discern whether two side-by-side pictures are the same or not, and measures the number of items correct in a 90-second period. The PCPS is appropriate for use across the lifespan (ages, 3–85 years) and has high construct validity (Carlozzi et al., 2014).

Diffusion data collection and preprocessing—Diffusion imaging data was collected at Washington University, St. Louis, using a customized Siemens Magnetom Connectome 3 Tesla scanner with a 100 mT/m maximum gradient strength and a 32 channel head coil. Details on the scanner, image acquisition and reconstruction reported elsewhere (Ugurbil et al., 2013) and are available online(https://www.humanconnectome.org/documentation/S500/HCP_S500_Release_Reference_Manual.pdf). Diffusion data were collected using a single-shot, single refocusing spin-echo, echo-planar imaging sequence with 1.25 mm isotropic spatial resolution (TE/TR=89.5/5520 ms, FOV=210×180 mm). Three gradient tables of 90 diffusion-weighted directions, and six b=0 images each, were collected with right-to-left and

left-to-right phase encoding polarities for each of the three diffusion weightings (b=1000, 2000, and 3000 s/mm^2). The total imaging time for collection of diffusion data was approximately one hour. Diffusion data were preprocessed using the HCP Diffusion pipeline (Glasser et al., 2013; Sotiropoulos et al., 2013) that included: normalization of b0 image intensity across runs; correction for EPI susceptibility and eddy-current-induced distortions, gradient-nonlinearities, subject motion and application of a brain mask. FA maps were obtained by fitting diffusion tensor model using FSL-FDT toolkit (Behrens et al., 2003).

Extraction of whole-brain average and regional FA values

ENIGMA-DTI protocols to extract whole-brain and tract-wise average FA values were used for both datasets. These protocols are detailed elsewhere (Jahanshad et al., 2013) and are available online, at http://enigma.ini.usc.edu/protocols/dti-protocols/. Briefly, FA images from HCP subjects were non-linearly registered to the ENIGMA-DTI target brain using FSL's FNIRT (Jahanshad et al., 2013). This target was created as a "minimal deformation target" based on images from the participating studies as previously described (Jahanshad et al., 2013). The data were then processed using FSL's tract-based spatial statistics (TBSS; http://fsl.fmrib.ox.ac.uk/fsl/fslwiki/TBSS) analytic method (Smith et al., 2006) modified to project individual FA values on the hand-segmented ENIGMA-DTI skeleton mask. After extracting the skeletonized white matter and the projection of individual FA values, ENIGMA tract-wise regions of interest, derived from the Johns Hopkins University (JHU) white matter parcellation atlas (Mori et al., 2008), were transferred to extract the mean FA across the full skeleton and average FA values for eleven major white matter tracts (**Table 1**). The whole brain average FA values were calculated to include all voxels in the ENIGMA-DTI skeleton. The protocol, target brain, ENIGMA-DTI skeleton mask, source code and executables, are all publicly available (http://enigma.ini.usc.edu/ongoing/dti-working-group/).

Heritability and genetic correlation analyses

We estimated the heritability (h^2) of FA values and brain processing speed as the proportion of the total phenotypic variance that can be explained by the additive effects of genes. Briefly, we modeled the observed phenotypic co-variance between each pair of individuals as having an expected value given by the product of their coefficient of relatedness (as defined by the pedigree structure) and the observed phenotypic variance of the trait (conditional on covariate effects). Parameter estimates including the heritability are assessed by maximum likelihood. The significance of the additive genetic effect (h^2) is assessed by the likelihood ratio test that compares the likelihood of a model that includes the family structure versus a model that does not. All analyses were performed using the SOLAR-Eclipse software package (http://www.nitrc.org/projects/se_linux).

To estimate the extent to which a common set of genes influences variation in brain processing speed and FA values jointly, we used classical quantitative genetic models to partition the phenotypic correlation between two phenotypes into a genetic and environmental components. Briefly, the phenotypic correlation can be partitioned into the genetic ρ_G, and environmental ρ_E components. For traits A and B this decomposition is

$$\rho_P = \sqrt{h_A^2} \sqrt{h_B^2} \cdot \rho_G + \sqrt{1 - h_A^2} \sqrt{1 - h_B^2} \cdot \rho_E, \quad (3)$$

where h_A^2 and h_B^2 denote the heritability for each trait. Thus, the shared variance is expressed using shared additive genetic effects and the residual environmental effects. To estimate the additive ρ_G and the random ρ_E for pairs of traits, the multivariate phenotype of an individual is modeled as a linear function of kinship coefficients that express relatedness among all pairs of individuals in the pedigree. Using standard quantitative genetic theory, the phenotypic variance-covariance matrix and its additive genetic and random environmental components are then obtained. From these matrices, the significance of the ρ_G and ρ_E are estimated directly by the likelihood ratio test (Almasy et al., 1997; Williams-Blangero and Blangero, 1992). This test compares the likelihood of a model in which additive and environmental components, in turn, are constrained to zero against the full model in which all parameters are estimated simultaneously. This provides the estimates for ρ_G and ρ_E and their standard error. The significance of these coefficients is determined by a z-test of difference from zero. If the ρ_G is significantly different from the zero then a significant proportion of the traits' covariance is considered to be influenced by shared genetic factors (Almasy and Blangero, 2010; Almasy et al., 1997).

All analyses were conducted with age, age^2, age $\times$ sex and age^2 $\times$ sex included as covariates. In OOA sample, psychotropic medication status was included as a binary covariate. Inverse Gaussian transformation was applied to ensure normality of the measures. The level of statistical significance for regional measurements was set at p=0.0045 to correct for multiple (N=11) comparisons. P-values in the interval of 0.0045<p 0.05 were defined as nominally significant and included into the discussion.

Results

Heritability analyses

Whole-brain FA and processing speed were significantly heritable in both cohorts (h^2 of whole-brain FA = 87% and 88% and h^2 of processing speed = 43% and 49% in OOA and HCP, respectively) (Table 1).

Heritability analysis of regional measurements of FA values in OOA sample demonstrated significant heritability (after correction for N=11 comparisons) in five tracts: the genu, body, and splenium of the corpus callosum, cingulum and superior longitudinal fasciculus (all p<0.003) (**Figure 1, Table 1**). Nominally significant (0.0045<p<0.05) heritability values were also observed for all other tracts, except for the fornix (FX) (**Table 1**).

In OOA sample age was the sole significant covariate (p<0.05) for whole brain average (p=0.01), all regional FA (0.05<p<0.001) values and processing speed (p=0.02). Medication status in OAA was included as a covariate and was shown to be non-significant in all heritability analyses (all p>0.2).

Heritability values for regional FA values in HCP data were taken from our previous work (Kochunov et al., 2015) and were significant in all tracts (Table 1). Age was a non-

significant covariate for either regional FA values or processing speed in HCP sample. There was a significant and positive correlation (r=0.75, p=0.02) between heritability estimates for regional FA measurements in the OOA and HCP cohorts (Figure 2).

Correlations between FA and processing speed

Significant phenotypic correlation (ρ_P) was observed between whole-brain average FA and processing speed (ρ_P=0.37, p=0.004). Significant phenotypic correlations were observed for the genu of CC and the sagittal stratum tracts (ρ_P=0.38, p=0.002 for both) (**Table 2**). Nominally significant ρ_P values were observed for the body and splenium of the corpus callosum, the *corona radiata* (CR) and superior longitudinal fasciculus (SLF) (**Figure 3, Table 3**).

Genetic correlation analyses in OAA sample demonstrated significant shared genetic variance between average FA and processing speed (ρ_G=0.63 ± 0.39, p=0.04). For regional FA values, although none of the coefficients achieved statistical significance at p<0.003, all genetic correlation coefficients were positive and nominally significant for the genu, splenium and fornix (**Figure 3, Table 3**). All environmental correlation coefficients were non-significant (all p>0.4).

In HCP sample, a positive and significant phenotypic correlation ρ_P was observed between average FA and processing speed (ρ_P=0.17 p=0.001). The ρ_P coefficient was numerically lower than that in OOA but there was no significant difference between them (z=1.70,p>0.1). Regionally, the ρ_P was significant for the SLF, cortico-spinal (CST) and SS tracts and nominally significant for the splenium of the corpus callosum and corona radiata (CR) (**Table 2**). The phenotypic correlation coefficients were smaller for HCP than for OOA, likely due to a smaller variance in the cognitive performance data (average processing speed ± std dev =60.0±18.9 vs. 111.8±12.0 for OOA and HCP, respectively) and in FA (whole brain FA: =0.365±0.021 vs. 0.399±0.012) (Table 1S, see supplement)

The ρ_P coefficients for regional FA measurements and processing speed in HCP were also not significantly different from these in OOA with exception for the genu of corpus callosum (p=0.02). The correlation between regional ρ_P values for OOA and HCP cohorts was positive and significant (r=0.62, p=0.04) (Figure 4, top).

Likewise, the genetic correlation analyses showed a significant correlation between whole-brain average FA and processing speed (ρ_G=0.32 ± 0.10, p=0.002). There were no significant differences in the genetic correlation coefficients between OOA and HCP samples (p=0.13). Significant ρ_G values were observed for the splenium, internal capsule (IC) and SS tracts (p 0.0045). Nominal significance was observed for the CR, external capsule (EC), SLF and CST tract (0.05>p>0.003). Nominally significant differences between OOA and HCP cohorts were only observed for the splenium of corpus callosum (p=0.03). All environmental correlation coefficients were non-significant (all p>0.4). The correlation between regional ρ_G was positive but not significant (r=0.45, p=0.16) (Table 3, Figure 4, bottom)

Discussion

We demonstrated a significant shared additive genetic contribution between intersubject variability in the processing speed and fractional anisotropy (FA) of cerebral WM. This finding was first observed in the Old Order Amish subjects and then replicated in data collected and distributed by the Human Connectome Project. This suggests that the common genetic effects significantly contribute to the phenotypic association between the two traits. This finding was observed despite the differences in the OOA and HCP family structure, sample size, age range, sociocultural background, and the imaging and processing speed assessment tools.

Both OOA and HCP are robust familial samples, although they also differ in several important aspects. The OOA cohort consisted of subjects ascertained from a large multigenerational pedigree. Farm-dwelling OOA subjects have higher environmental homogeneity compared to the urban/suburban HCP sample. OOA are perhaps best known for their old-fashioned dress and resistance to technological change. OOA share rural upbringing and similar diet, income and work environment. All OOA receive uniform 8th grade level education. Illicit drug use was not present in our sample. In comparison, the HCP sample consisted of twin-pairs and siblings with diverse ethnic and economic backgrounds. Other distinct features include the age range. The OOA subjects were recruited across the lifespan (age rage=18-75) and heritability analyses identified age as a significant covariate for both processing speed and FA values. The HCP recruitment was focused on a narrow age range from 22 to 35 years that corresponds to the plateau in the FA and processing speed aging trends (Kochunov et al., 2011; Van Essen et al., 2013). The lack of aging-related trends in FA values were already reported in HCP (Kochunov et al., 2014). Likewise, we found no impact of subjects' age on the processing speed measurements in HCP sample (p>0.1). Thus, the OOA and HCP samples differ in environmental and likely population genetic contribution, making the similar findings in heritability and genetic correlation more convincing.

Despite the difference in imaging methods, the heritability estimates for the whole-brain average FA values were similar (h^2=0.87 vs. 0.88) for OOA and HCP cohorts. Likewise, the tract-wise average FA values in OOA and HCP subjects showed a good agreement (r=0.75). Heritability is the proportion of the variance that is attributed to the additive genetic variance after correction for covariates. In OOA sample age was the only significant covariate. The HCP sample show no age effect likely because the recruitment strategy was designed to reduce the effects of age on the brain measurements by limiting age-range to that corresponds to a plateau in FA-aging trend (22-35 years) (Kochunov et al., 2011; Van Essen et al., 2013).

Another source of variability is the difference in methods used to ascertain processing speed in OOA and HCP samples. The digit-symbol coding test used in the OOA sample is a standard neurocognitive assessment tool to assess processing speed, commonly used in psychiatric research(Knowles et al., 2010). The processing speed in the HCP sample was measured using the pattern comparison processing speed test. Both tests are accepted measurements of processing speed and share between 30-40% of the intersubject

variance(Carlozzi et al., 2014; Carlozzi et al., 2013). Despite differences in processing speed tasks in the OOA and HCP cohorts, we found only sporadic differences in phenotypic and genetic correlations across samples; these differences however, were not statistically significant after correction for multiple compassions. The fact that phenotypic and genetic correlation coefficients were positively correlated between the two samples supports the notion that shared variance between FA values and processing speed are not specific to a behavioral task or a particular population.

We believe the difference in processing speed measurement tests rather than the imaging protocol may to a greater extent explain why the correlation coefficients in OOA subjects were numerically higher than these in HCP cohort. While, this difference was not significant for the whole-brain average FA values, it was nominally significant for the genu and splenium of corpus callosum for the phenotypic and genetic correlation, respectively. In OOA, the phenotypic correlation between FA values of the genu and processing speed were statistically significant (r=0.38, p=0.003). In comparison, in HCP sample this correlation was only suggestively significant (r=0.09, p=0.06). In the same time, there was no significant difference for the heritability estimate for the FA for this structure (h^2=0.76 vs. 0.89, for OOA and HCP, respectively, p=0.17). The genu contains the primary fibers connecting the left and right frontal lobes and the genetic contribution to processing speed may in part be through genetic influence on the speed of frontal lobe communication (Aboitiz, 1992; Aboitiz et al., 1992; Bartzokis et al., 2010). Normal aging and lesion studies suggest that the decision making process in the digit symbol coding task is sensitive to the structural integrity of the frontal white matter, regardless of variance in reaction time(Kochunov et al., 2010; Leavitt et al., 2011; Raji et al., 2012). Instead, the pattern of correlation in the HCP had a more posterior/inferior bias with the highest correlations in the corticospinal (CST) and the sagittal stratum (SS) areas with the PCPS processing speed task. The PCPS test has a heavy visual loading, which may explain the heavy loading on WM structures that serve visual-spatial subsystems including the splenium of corpus callosum (SCC) and SS. Notably, the phenotypic correlation for these structures were also nominally significant in OOA sample. Genetic correlation coefficients were nominally different for the splenium of corpus callosum, with higher ρ_G values observed in OOA sample (ρ_G =0.76 vs 0.26 in OOA and HCP respectively). Nonetheless, both coefficients were significantly different from zero in OOA and HCP cohorts (p=0.02 and 0.005 in OOA and HCP, respectively). Therefore, the differences in the loading of the digit symbol vs. PCPS processing speed tests on specific cognitive domains is the likely explanation of the numerical differences in the phenotypic and genetic correlation coefficients between OOA and HCP cohorts.

A potential limitation of this study is the use of psychiatric drugs by N=22 OOA subjects, with a lifetime diagnosis of mental illness that may have potentially affected brain structure. The use of psychiatric drug was coded as a binary covariate during all analyses. However, as this covariate was robustly non-significant, we believe it to be a minor limitation. Another limitation of this study is that we did not collect peripheral pulse oximetry data during the DTI acquisition. Advanced DTI reconstruction techniques allow for use of peripheral data such as pulse and respiration to improve signal-to-noise ratio in tensor fit, especially in the areas of brainstem and cerebellum (Mohammadi et al., 2013). In the absence of cardiac

gating during the acquisition, it is also possible to vet or edit the input data with publicly available software that allows removal of outliers or volumes corrupted by excessive movement from the tensor calculation, although we did not use such an approach in this study.

Overall, our findings imply that specific genes influencing variance in FA values may also exert influence over the speed of cognitive information processing. This finding is of importance for neuropsychiatric disorders such as schizophrenia where the reduced speed of information processing and reduced cerebral FA values are highly replicable findings and believed to be interlinked (Alba-Ferrara and de Erausquin, 2013; Ellison-Wright and Bullmore, 2009; Friedman et al., 2008; Glahn et al., 2013; Kubicki et al., 2007; Nazeri et al., 2012; Penke et al., 2010; Perez-Iglesias et al., 2011; Phillips et al., 2012). Together, our results support common sets of genes influencing variation in processing speed and white matter FA phenotypes, consistent with the idea of pleiotropic effects in brain structure and cognitive behavior. Our findings may pave a way for multivariate genetic localization analyses that combine processing speed and FA-values to directly identify genes that may have impact in multiple psychiatric disorders.

Supplementary Material

Refer to Web version on PubMed Central for supplementary material.

Acknowledgments

Reference

Aboitiz F. Brain connections: interhemispheric fiber systems and anatomical brain asymmetries in humans. Biol Res. 1992; 25:51–61. [PubMed: 1365702]

Aboitiz F, Scheibel AB, Fisher RS, Zaidel E. Fiber composition of the human corpus callosum. Brain Res. 1992; 598:143–153. [PubMed: 1486477]

Agarwala R, Biesecker LG, Tomlin JF, Schaffer AA. Towards a complete North American Anabaptist genealogy: A systematic approach to merging partially overlapping genealogy resources. Am J Med Genet. 1999; 86:156–161. [PubMed: 10449652]

Alba-Ferrara LM, de Erausquin GA. What does anisotropy measure? Insights from increased and decreased anisotropy in selective fiber tracts in schizophrenia. Front Integr Neurosci. 2013; 7:9. [PubMed: 23483798]

Almasy L, Blangero J. Variance Component Methods for Analysis of Complex Phenotypes. Cold Spring Harbor protocols 2010. 2010:pdb.top77–pdb.top77.

Almasy L, Dyer TD, Blangero J. Bivariate quantitative trait linkage analysis: pleiotropy versus co-incident linkages. Genet Epidemiol. 1997; 14:953–958. [PubMed: 9433606]

Bartzokis G. Age-related myelin breakdown: a developmental model of cognitive decline and Alzheimer's disease. Neurobiol Aging. 2004; 25:5–18. [PubMed: 14675724]

Bartzokis G, Lu PH, Tingus K, Mendez MF, Richard A, Peters DG, Oluwadara B, Barrall KA, Finn JP, Villablanca P, Thompson PM, Mintz J. Lifespan trajectory of myelin integrity and maximum motor speed. Neurobiol Aging. 2008

Bartzokis G, Lu PH, Tingus K, Mendez MF, Richard A, Peters DG, Oluwadara B, Barrall KA, Finn JP, Villablanca P, Thompson PM, Mintz J. Lifespan trajectory of myelin integrity and maximum motor speed. Neurobiology of aging. 2010; 31:1554–1562. [PubMed: 18926601]

Basser PJ. Focal magnetic stimulation of an axon. IEEE Transactions on Biomedical Engineering. 1994; 41:601–606. [PubMed: 7927380]

Beaulieu C. The basis of anisotropic water diffusion in the nervous system - a technical review. NMR Biomed. 2002; 15:435–455. [PubMed: 12489094]

Behrens TE, Woolrich MW, Jenkinson M, Johansen-Berg H, Nunes RG, Clare S, Matthews PM, Brady JM, Smith SM. Characterization and propagation of uncertainty in diffusion-weighted MR imaging. Magn Reson Med. 2003; 50:1077–1088. [PubMed: 14587019]

Braskie MN, Jahanshad N, Stein JL, Barysheva M, McMahon KL, de Zubicaray GI, Martin NG, Wright MJ, Ringman JM, Toga AW, Thompson PM. Common Alzheimer's disease risk variant within the CLU gene affects white matter microstructure in young adults. J Neurosci. 2011; 31:6764–6770. [PubMed: 21543606]

Carlozzi NE, Tulsky DS, Chiaravalloti ND, Beaumont JL, Weintraub S, Conway K, Gershon RC. NIH Toolbox Cognitive Battery (NIHTB-CB): the NIHTB Pattern Comparison Processing Speed Test. J Int Neuropsychol Soc. 2014; 20:630–641. [PubMed: 24960594]

Carlozzi NE, Tulsky DS, Kail RV, Beaumont JL. VI. NIH Toolbox Cognition Battery (CB): measuring processing speed. Monogr Soc Res Child Dev. 2013; 78:88–102. [PubMed: 23952204]

Charlton RA, Schiavone F, Barrick TR, Morris RG, Markus HS. Diffusion Tensor Imaging detects age-related white matter change over a two-year follow-up which is associated with working memory decline. Journal of neurology, neurosurgery, and psychiatry. 2009

Chiang MC, Barysheva M, McMahon KL, de Zubicaray GI, Johnson K, Montgomery GW, Martin NG, Toga AW, Wright MJ, Shapshak P, Thompson PM. Gene network effects on brain microstructure and intellectual performance identified in 472 twins. J Neurosci. 2012; 32:8732–8745. [PubMed: 22723713]

Chiang MC, Barysheva M, Shattuck DW, Lee AD, Madsen SK, Avedissian C, Klunder AD, Toga AW, McMahon KL, de Zubicaray GI, Wright MJ, Srivastava A, Balov N, Thompson PM. Genetics of brain fiber architecture and intellectual performance. J Neurosci. 2009; 29:2212–2224. [PubMed: 19228974]

Conturo TE, McKinstry RC, Akbudak E, Robinson BH. Encoding of anisotropic diffusion with tetrahedral gradients: a general mathematical diffusion formalism and experimental results. Magn Reson Med. 1996; 35:399–412. [PubMed: 8699953]

Edens EL, Glowinski AL, Pergadia ML, Lessov-Schlaggar CN, Bucholz KK. Nicotine addiction in light smoking African American mothers. J Addict Med. 2010; 4:55–60. [PubMed: 20582148]

Ellison-Wright I, Bullmore E. Meta-analysis of diffusion tensor imaging studies in schizophrenia. Schizophr Res. 2009; 108:3–10. [PubMed: 19128945]

Felts PA, Baker TA, Smith KJ. Conduction in segmentally demyelinated mammalian central axons. J Neurosci. 1997; 17:7267–7277. [PubMed: 9295373]

Flechsig P. Developmental (myelogenetic) localisation of the cerebral cortex in the human. Lancet. 1901; 158:1027–1030.

Friedman JI, Tang C, Carpenter D, Buchsbaum M, Schmeidler J, Flanagan L, Golembo S, Kanellopoulou I, Ng J, Hof PR, Harvey PD, Tsopelas ND, Stewart D, Davis KL. Diffusion tensor imaging findings in first-episode and chronic schizophrenia patients. Am J Psychiatry. 2008; 165:1024–1032. [PubMed: 18558643]

Glahn DC, Curran JE, Winkler AM, Carless MA, Kent JW Jr. Charlesworth JC, Johnson MP, Goring HH, Cole SA, Dyer TD, Moses EK, Olvera RL, Kochunov P, Duggirala R, Fox PT, Almasy L, Blangero J. High Dimensional Endophenotype Ranking in the Search for Major Depression Risk Genes. Biol Psychiatry. 2011; 71:6–14. [PubMed: 21982424]

Glahn DC, Kent JW Jr. Sprooten E, Diego VP, Winkler AM, Curran JE, McKay DR, Knowles EE, Carless MA, Goring HH, Dyer TD, Olvera RL, Fox PT, Almasy L, Charlesworth J, Kochunov P, Duggirala R, Blangero J. Genetic basis of neurocognitive decline and reduced white-matter integrity in normal human brain aging. Proc Natl Acad Sci U S A. 2013; 110:19006–19011. [PubMed: 24191011]

Glasser MF, Sotiropoulos SN, Wilson JA, Coalson TS, Fischl B, Andersson JL, Xu J, Jbabdi S, Webster M, Polimeni JR, Van Essen DC, Jenkinson M. The minimal preprocessing pipelines for the Human Connectome Project. Neuroimage. 2013; 80:105–124. [PubMed: 23668970]

Jahanshad N, Kochunov P, Sprooten E, Mandl RC, Nichols TE, Almassy L, Blangero J, Brouwer RM, Curran JE, de Zubicaray GI, Duggirala R, Fox PT, Hong LE, Landman BA, Martin NG, McMahon KL, Medland SE, Mitchell BD, Olvera RL, Peterson CP, Starr JM, Sussmann JE, Toga AW, Wardlaw JM, Wright MJ, Hulshoff Pol HE, Bastin ME, McIntosh AM, Deary IJ, Thompson PM, Glahn DC. Multi-site genetic analysis of diffusion images and voxelwise heritability analysis: A pilot project of the ENIGMA-DTI working group. Neuroimage. 2013 doi:pii: S1053-8119(13)00408-4. 10.1016/j.neuroimage.2013.04.061.

Jahanshad N, Kohannim O, Hibar DP, Stein JL, McMahon KL, de Zubicaray GI, Medland SE, Montgomery GW, Whitfield JB, Martin NG, Wright MJ, Toga AW, Thompson PM. Brain structure in healthy adults is related to serum transferrin and the H63D polymorphism in the HFE gene. Proc Natl Acad Sci U S A. 2012; 109:E851–859. [PubMed: 22232660]

Jahanshad N, Lee AD, Barysheva M, McMahon KL, de Zubicaray GI, Martin NG, Wright MJ, Toga AW, Thompson PM. Genetic influences on brain asymmetry: a DTI study of 374 twins and siblings. Neuroimage. 2010; 52:455–469. [PubMed: 20430102]

Jones DK, Horsfield MA, Simmons A. Optimal strategies for measuring diffusion in anisotropic systems by magnetic resonance imaging. Magn Reson Med. 1999; 42:515–525. [PubMed: 10467296]

Jones DK, Knosche TR, Turner R. White matter integrity, fiber count, and other fallacies: the do's and don'ts of diffusion MRI. Neuroimage. 2013; 73:239–254. [PubMed: 22846632]

Karbasforoushan H, Duffy B, Blackford JU, Woodward ND. Processing speed impairment in schizophrenia is mediated by white matter integrity. Psychol Med. 2015; 45:109–120. [PubMed: 25066842]

Kennedy KM, Raz N. Aging white matter and cognition: differential effects of regional variations in diffusion properties on memory, executive functions, and speed. Neuropsychologia. 2009; 47:916–927. [PubMed: 19166865]

Kessler RC, Demler O, Frank RG, Olfson M, Pincus HA, Walters EE, Wang P, Wells KB, Zaslavsky AM. Prevalence and treatment of mental disorders, 1990 to 2003. N Engl J Med. 2005; 352:2515–2523. [PubMed: 15958807]

Knowles EE, David AS, Reichenberg A. Processing speed deficits in schizophrenia: reexamining the evidence. The American journal of psychiatry. 2010; 167:828–835. [PubMed: 20439390]

Kochunov P, Coyle T, Lancaster J, Hardies J, Kochunov V, Bartzokis G, Royall D, Stanley J, Schlosser A, Fox P. Processing speed is correlated with cerebral health markers in the frontal lobes as quantified by neuro-imaging. Neuroimage. 2009a In press.

Kochunov P, Coyle T, Lancaster J, Robin DA, Hardies J, Kochunov V, Bartzokis G, Stanley J, Royall D, Schlosser AE, Null M, Fox PT. Processing speed is correlated with cerebral health markers in the frontal lobes as quantified by neuroimaging. Neuroimage. 2010; 49:1190–1199. [PubMed: 19796691]

Kochunov P, Glahn DC, Lancaster J, Thompson PM, Kochunov V, Rogers B, Fox P, Blangero J, Williamson DE. Fractional anisotropy of cerebral white matter and thickness of cortical gray matter across the lifespan. Neuroimage. 2011; 58:41–49. [PubMed: 21640837]

Kochunov P, Jahanshad N, Marcus D, Winkler A, Sproote E, Nichols T, Hong L, Behrens TE, Andersson J, Yacoub E, Ugurbil K, Brouwer C, Landman BA, Braber A, Almassy L, Fox PT, Olvera R, Blangero J, DC. G, Van Essen DC. Heritability of Fractional Anisotropy in Human White Matter: A Comparison of Human Connectome Project and ENIGMA-DTI Data. Neuroimage. 2014 In Review.

Kochunov P, Jahanshad N, Marcus D, Winkler A, Sprooten E, Nichols TE, Wright SN, Hong LE, Patel B, Behrens T, Jbabdi S, Andersson J, Lenglet C, Yacoub E, Moeller S, Auerbach E, Ugurbil K, Sotiropoulos SN, Brouwer RM, Landman B, Lemaitre H, den Braber A, Zwiers MP, Ritchie S, van Hulzen K, Almasy L, Curran J, deZubicaray GI, Duggirala R, Fox P, Martin NG, McMahon KL, Mitchell B, Olvera RL, Peterson C, Starr J, Sussmann J, Wardlaw J, Wright M, Boomsma DI, Kahn R, de Geus EJ, Williamson DE, Hariri A, van 't Ent D, Bastin ME, McIntosh A, Deary IJ, Hulshoff Pol HE, Blangero J, Thompson PM, Glahn DC, Van Essen DC. Heritability of fractional

anisotropy in human white matter: A comparison of Human Connectome Project and ENIGMA-DTI data. Neuroimage. 2015; 111:300–311. [PubMed: 25747917]

Kochunov P, Robin D, Royall D, Lancaster J, Kochunov V, Coyle T, Schlosser A, Fox P. Can structural MRI cerebral health markers track cognitive trends in executive control function during normal maturation and adulthood? Hum Brain Mapp. 2009b; 30:2581–2594. [PubMed: 19067326]

Kochunov P, Williamson DE, Lancaster J, Fox P, Cornell J, Blangero J, Glahn DC. Fractional anisotropy of water diffusion in cerebral white matter across the lifespan. Neurobiol Aging. 2012; 33:9–20. [PubMed: 20122755]

Konrad A, Vucurevic G, Musso F, Stoeter P, Winterer G. Correlation of Brain White Matter Diffusion Anisotropy and Mean Diffusivity with Reaction Time in an Oddball Task. Neuropsychobiology. 2009; 60:55–66. [PubMed: 19752579]

Kubicki M, McCarley R, Westin CF, Park HJ, Maier S, Kikinis R, Jolesz FA, Shenton ME. A review of diffusion tensor imaging studies in schizophrenia. J Psychiatr Res. 2007; 41:15–30. [PubMed: 16023676]

Leavitt VM, Wylie G, Genova HM, Chiaravalloti ND, DeLuca J. Altered effective connectivity during performance of an information processing speed task in multiple sclerosis. Mult Scler. 2011; 18:409–417. [PubMed: 21965419]

Marcus DS, Harms MP, Snyder AZ, Jenkinson M, Wilson JA, Glasser MF, Barch DM, Archie KA, Burgess GC, Ramaratnam M, Hodge M, Horton W, Herrick R, Olsen T, McKay M, House M, Hileman M, Reid E, Harwell J, Coalson T, Schindler J, Elam JS, Curtiss SW, Van Essen DC. Human Connectome Project informatics: quality control, database services, and data visualization. Neuroimage. 2013; 80:202–219. [PubMed: 23707591]

Mohammadi S, Hutton C, Nagy Z, Josephs O, Weiskopf N. Retrospective correction of physiological noise in DTI using an extended tensor model and peripheral measurements. Magn Reson Med. 2013; 70:358–369. [PubMed: 22936599]

Muetzel RL, Collins PF, Mueller BA, A MS, Lim KO, Luciana M. The development of corpus callosum microstructure and associations with bimanual task performance in healthy adolescents. Neuroimage. 2008; 39:1918–1925. [PubMed: 18060810]

Nazeri A, Mallar Chakravarty M, Felsky D, Lobaugh NJ, Rajji TK, Mulsant BH, Voineskos AN. Alterations of Superficial White Matter in Schizophrenia and Relationship to Cognitive Performance. Neuropsychopharmacology. 2012

Penke L, Munoz Maniega S, Murray C, Gow AJ, Hernandez MC, Clayden JD, Starr JM, Wardlaw JM, Bastin ME, Deary IJ. A general factor of brain white matter integrity predicts information processing speed in healthy older people. J Neurosci. 2010; 30:7569–7574. [PubMed: 20519531]

Perez-Iglesias R, Tordesillas-Gutierrez D, McGuire PK, Barker GJ, Roiz-Santianez R, Mata I, de Lucas EM, Rodriguez-Sanchez JM, Ayesa-Arriola R, Vazquez-Barquero JL, Crespo-Facorro B. White matter integrity and cognitive impairment in first-episode psychosis. Am J Psychiatry. 2011; 167:451–458. [PubMed: 20160006]

Phillips KA, Rogers J, Barrett EA, Glahn DC, Kochunov P. Genetic contributions to the midsagittal area of the corpus callosum. Twin Res Hum Genet. 2012; 15:315–323. [PubMed: 22856367]

Pierpaoli C, Basser PJ. Toward a quantitative assessment of diffusion anisotropy. Magn Reson Med. 1996; 36:893–906. [PubMed: 8946355]

Raji CA, Lopez OL, Kuller LH, Carmichael OT, Longstreth WT Jr. Gach HM, Boardman J, Bernick CB, Thompson PM, Becker JT. White matter lesions and brain gray matter volume in cognitively normal elders. Neurobiol Aging. 2012; 33:834 e837–816. [PubMed: 21943959]

Salthouse TA. When does age-related cognitive decline begin? Neurobiol Aging. 2009; 30:507–514. [PubMed: 19231028]

Sartor CE, McCutcheon VV, Pommer NE, Nelson EC, Grant JD, Duncan AE, Waldron M, Bucholz KK, Madden PA, Heath AC. Common genetic and environmental contributions to post-traumatic stress disorder and alcohol dependence in young women. Psychol Med. 2010; 41:1497–1505. [PubMed: 21054919]

Schiavone F, Charlton RA, Barrick TR, Morris RG, Markus HS. Imaging age-related cognitive decline: A comparison of diffusion tensor and magnetization transfer MRI. J Magn Reson Imaging. 2009; 29:23–30. [PubMed: 19097099]

Shen KK, Rose S, Fripp J, McMahon KL, de Zubicaray GI, Martin NG, Thompson PM, Wright MJ, Salvado O. Investigating brain connectivity heritability in a twin study using diffusion imaging data. Neuroimage. 2014; 100:628–641. [PubMed: 24973604]

Smith SM. Fast robust automated brain extraction. Hum Brain Mapp. 2002; 17:143–155. [PubMed: 12391568]

Smith SM, Jenkinson M, Johansen-Berg H, Rueckert D, Nichols TE, Mackay CE, Watkins KE, Ciccarelli O, Cader MZ, Matthews PM, Behrens TE. Tract-based spatial statistics: Voxelwise analysis of multi-subject diffusion data. Neuroimage. 2006; 31:1487–1505. [PubMed: 16624579]

Sotiropoulos SN, Jbabdi S, Xu J, Andersson JL, Moeller S, Auerbach EJ, Glasser MF, Hernandez M, Sapiro G, Jenkinson M, Feinberg DA, Yacoub E, Lenglet C, Van Essen DC, Ugurbil K, Behrens TE. Advances in diffusion MRI acquisition and processing in the Human Connectome Project. Neuroimage. 2013; 80:125–143. [PubMed: 23702418]

Ugurbil K, Xu J, Auerbach EJ, Moeller S, Vu AT, Duarte-Carvajalino JM, Lenglet C, Wu X, Schmitter S, Van de Moortele PF, Strupp J, Sapiro G, De Martino F, Wang D, Harel N, Garwood M, Chen L, Feinberg DA, Smith SM, Miller KL, Sotiropoulos SN, Jbabdi S, Andersson JL, Behrens TE, Glasser MF, Van Essen DC, Yacoub E, Consortium WU-MH. Pushing spatial and temporal resolution for functional and diffusion MRI in the Human Connectome Project. Neuroimage. 2013; 80:80–104. [PubMed: 23702417]

Ulug AM, Barker PB, van Zijl PC. Correction of motional artifacts in diffusion-weighted images using a reference phase map. Magn Reson Med. 1995; 34:476–480. [PubMed: 7500889]

Van Essen DC, Ugurbil K, Auerbach E, Barch D, Behrens TE, Bucholz R, Chang A, Chen L, Corbetta M, Curtiss SW, Della Penna S, Feinberg D, Glasser MF, Harel N, Heath AC, Larson-Prior L, Marcus D, Michalareas G, Moeller S, Oostenveld R, Petersen SE, Prior F, Schlaggar BL, Smith SM, Snyder AZ, Xu J, Yacoub E. The Human Connectome Project: a data acquisition perspective. Neuroimage. 2013; 62:2222–2231. [PubMed: 22366334]

Vernooij MW, Ikram MA, Vrooman HA, Wielopolski PA, Krestin GP, Hofman A, Niessen WJ, Van der Lugt A, Breteler MM. White matter microstructural integrity and cognitive function in a general elderly population. Arch Gen Psychiatry. 2009; 66:545–553. [PubMed: 19414714]

Waxman SG, Bennett MV. Relative conduction velocities of small myelinated and non-myelinated fibres in the central nervous system. Nat New Biol. 1972; 238:217–219. [PubMed: 4506206]

Wechsler, D. Wechsler Adult Intelligence Scale. 3rd edn.. Psychological Corporation; San Antonio, TX: 1997.

Williams-Blangero S, Blangero J. Quantitative genetic analysis of skin reflectance: a multivariate approach. Hum Biol. 1992; 64:35–49. [PubMed: 1582647]

Wright SN, Hong LE, Winkler AM, Chiappelli J, Nugent K, Muellerklein F, Du X, Rowland LM, Wang DJ, Kochunov P. Perfusion shift from white to gray matter may account for processing speed deficits in schizophrenia. Hum Brain Mapp. 2015
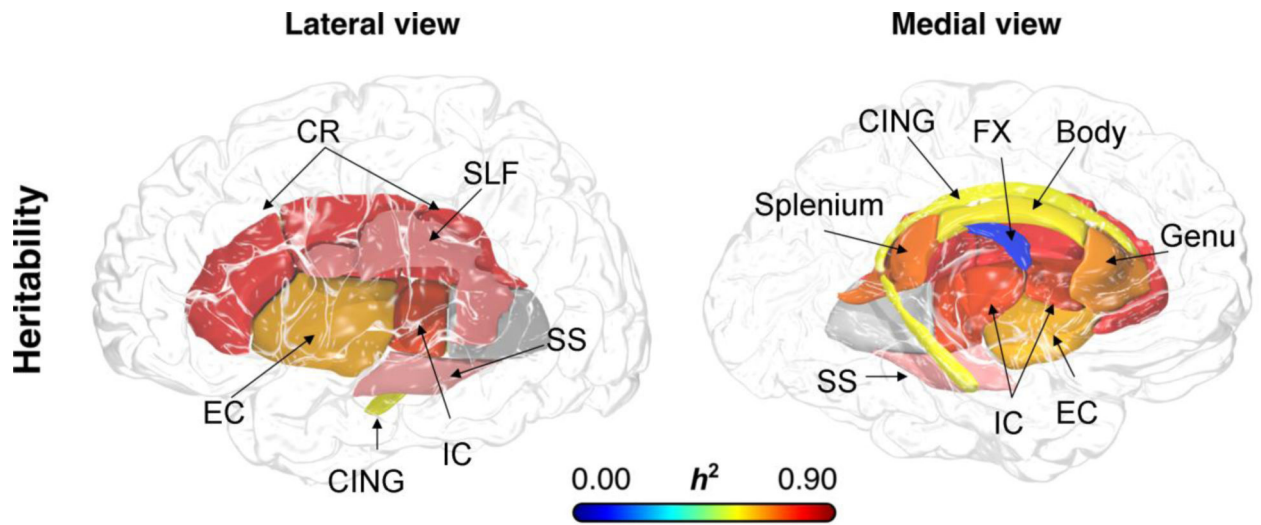
Figure 1.
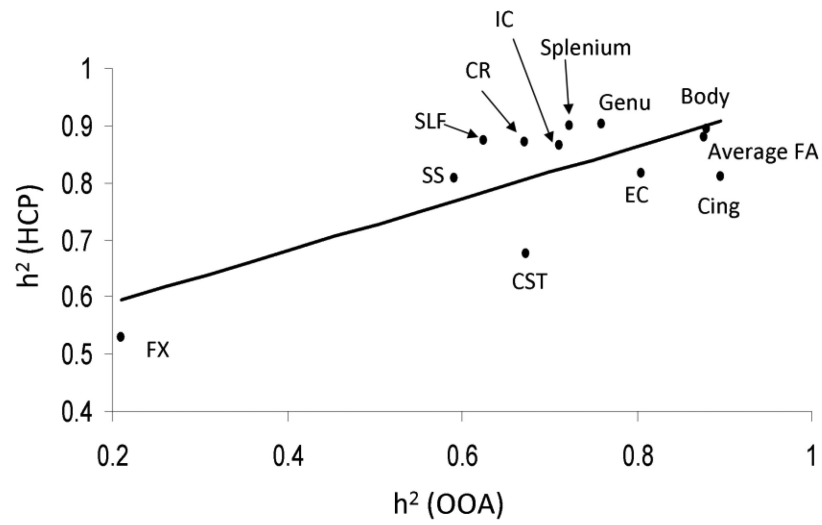Heritability of FA measurement for OOA sample.

Figure 2.
Heritability estimates for DTI-FA measured in OOA are presented as a scatter plot versus heritability estimates calculated in the HCP cohorts. The line represent the result of the linear correlation analysis between two cohorts that reported a positive and significant correlation r=0.75, p=0.02.
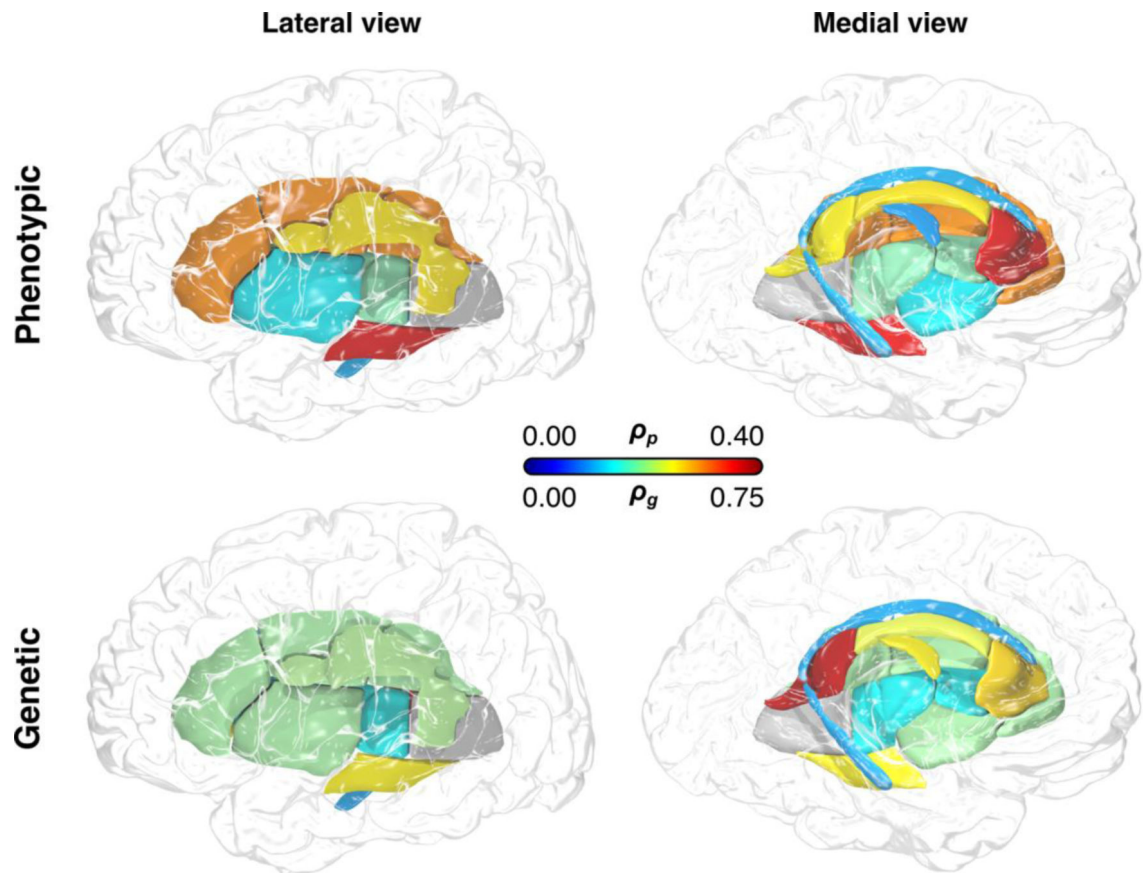
Figure 3.
Phenotypic (ρp), top row, and genetic (ρG), bottom row, correlation between of FA and processing speed measurement for OOA sample.

Figure 4.
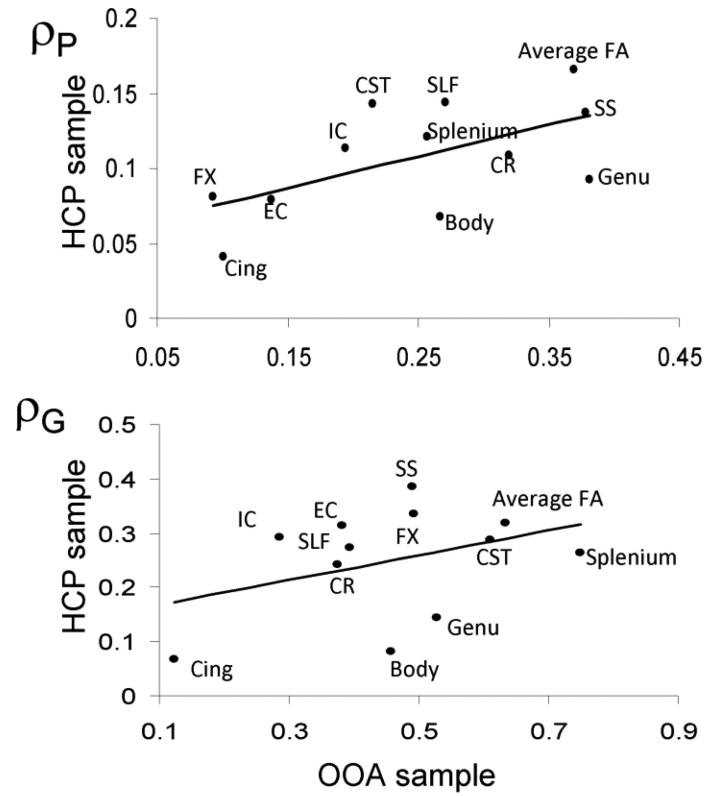A scatter plot of ρ_P (top panel) and ρ_G (bottom panel) values between DTI-FA and processing speed measurements in OOA and HCP cohorts. The lines represent the result of the linear correlation analysis between two cohorts. The positive correlation for ρ_p coefficients was significant r=0.62, p=0.04. The positive correlation ρ_G for was not significant (r=0.45, p=0.16).

Table 1

Heritability of processing speed and FA values in Amish and HCP populations.

Global phenotypes	OOA	HCP
Processing speed	**0.43±0.20 (p=0.005)**	**0.49±0.09 (p=2×10⁻⁶)**
Whole-brain average FA	**0.87±0.24 (p=6×10⁷)**	**0.88±0.03 (p=1×10⁻²⁵)**
Regional FA values		
Genu of the corpus callosum	**0.76+0.28 (p=0.002)**	**0.89±0.02 (p=1×10⁻³⁰)** [*]
Body of the corpus callosum	**0.88+0.26 (p=0.001** [*]**)**	**0.90±0.02 (p=1×10⁻²⁵)** [*]
Splenium of corpus callosum	**0.72+0.28 (p=0.003)** [*]	**0.90±0.02 (p=1×10⁻²⁶)** [*]
Fornix (FX)	0.21+0.26 (p=0.198)	**0.53±0.08 (p=1×10⁻⁹)** [*]
Cingulum (cingulate gyrus) - L and R combined (Cing)	**0.90+0.30 (p=0.001)** [*]	**0.81±0.04 (p=1×10⁻²²)** [*]
Corona radiata - L and R anterior, superior and posterior sections combined (CR)	**0.67+0.26 (p=0.018)**	**0.87±0.03 (p=1×10⁻²³)** [*]
External capsule - L and R combined (EC)	**0.80+0.32 (p=0.011)**	**0.82±0.05 (p=1×10⁻¹⁵)** [*]
Internal capsule - L and R anterior limb, posterior limb, and retrolenticular parts combined (IC)	**0.71+0.31 (p=0.009)**	**0.86±0.03 (p=1×10⁻²⁸)** [*]
Superior longitudinal fasciculus - L and R combined (SLF)	**0.62+0.25 (p=0.002)** [*]	**0.87±0.03 (p=1×10⁻²⁸)** [*]
Sagittal stratum (include inferior longitudinal fasciculus and inferior fronto-occipital fasciculus) - L and R combined (SS)	**0.59+0.29 (p=0.027)**	**0.81±0.05 (p=1×10⁻¹⁹)** [*]
Corticospinal tract - L and R combined (CST)	0.67+0.37 (p=0.08)	**0.66±0.05 (p=1×10⁻¹⁸)** [*]

Analyses in both cohorts were corrected for age, age^2, age×sex and age^2×sex. Bolded values are significant at p 0.05.

[*] Values that are significant after correction for multiple (N=11) comparisons.

Table 2

Phenotypic correlation coefficients (ρ_P) between processing speed and FA value (corrected for age, age2, age×sex and age2×sex).

Trait	OOA	HCP
Whole-brain Average FA	**0.37 (p=0.004)**	**0.17 (p=0.001)**
Regional FA values		
Genu of the corpus callosum	**0.38 (p=0.002)**[*]	0.09 (p=0.06)
Body of the corpus callosum	**0.27 (p=0.04)**	0.07 (p=0.18)
Splenium of corpus callosum	**0.26 (p=0.05)**	**0.12 (p=0.01)**
Fornix (FX)	0.09 (p=0.20)	0.08 (p=0.09)
Cingulum (cingulate gyrus) - L and R combined (Cing)	0.10 (p=0.20)	0.04 (p=0.41)
Corona radiata - L and R anterior, superior and posterior sections combined (CR)	**0.32 (p=0.004**[*]**)**	**0.11 (p=0.03)**
External capsule - L and R combined (EC)	0.14 (p=0.30)	0.08 (p=0.12)
Internal capsule - L and R anterior limb, posterior limb, and retrolenticular parts combined (IC)	0.19 (p=0.14)	**0.11 (p=0.02)**
Superior longitudinal fasciculus - L and R combined (SLF)	**0.27 (p=0.02)**	**0.13 (p=0.003)**[*]
Sagittal stratum (include inferior longitudinal fasciculus and inferior fronto-occipital fasciculus) - L and R combined (SS)	**0.38 (p=0.002)**[*]	**0.14 (p=0.005)**
Corticospinal tract - L and R combined (CST)	0.19 (p=0.22)	**0.15 (p=0.003)**[*]

Bolded values are significant at p 0.05.

[*] Values that are significant after correction for multiple (N=11) comparisons.

Table 3

Genetic correlation coefficients (ρ_G) between processing speed and FA value (corrected for age, age2, age×sex and age2×sex).

Trait	OOA	HCP
Whole-brain Average FA	**0.63 ± 0.39 (p=0.04)**	**0.32 ± 0.10 (p=0.002)**
Regional FA values		
Genu of the corpus callosum	**0.53 ± 0.33 (p=0.04)**	0.14 ± 0.10 (p=0.14)
Body of the corpus callosum	0.45 ± 0.43 (p=0.20)	0.08 ± 0.10 (p=0.41)
Splenium of corpus callosum	**0.75 ± 0.31 (p=0.02)**	**0.26 ± 0.09 (p=0.005)**
Fornix (FX)	**0.49 ± 0.19 (p=0.05)**	**0.33 ± 0.15 (p=0.021)**
Cingulum (cingulate gyrus) - L and R combined (Cing)	0.18 ± 0.42 (p=0.09)	0.07 ± 0.11 (p=0.538)
Corona radiata - L and R anterior, superior and posterior sections combined (CR)	0.38 ± 0.44 (p=0.45)	**0.24 ± 0.11 (p=0.02)**
External capsule - L and R combined (EC)	0.38 ± 0.32 (p=0.20)	**0.31 ± 0.12 (p=0.005)**
Internal capsule - L and R anterior limb, posterior limb, and retrolenticular parts combined (IC)	0.28 ± 0.48 (p=0.50)	**0.29 ± 0.10 (p=0.003)**[*]
Superior longitudinal fasciculus - L and R combined (SLF)	0.39 ± 0.31 (p=0.28)	**0.27 ± 0.10 (p=0.006)**
Sagittal stratum (include inferior longitudinal fasciculus and inferior fronto-occipital fasciculus) - L and R combined (SS)	0.49 ± 0.23 (p=0.07)	**0.39 ± 0.11 (p=0.0001)**[*]
Corticospinal tract - L and R combined (CST)	0.61 ± 0.64 (p=0.29)	**0.29 ± 0.11 (p=0.01)**

Bolded values are significant at p 0.05.

[*] Values that are significant after correction for multiple (N=11) comparisons.